

## NOTES AND CORRESPONDENCE

## Wave-Induced Effect on the Reynolds Shear Stress and Heat Flux in the Marine Surface Layer

A. J. CHAMBERS AND R. A. ANTONIA

*Department of Mechanical Engineering, University of Newcastle, N.S.W., 2308, Australia*

27 May 1980 and 10 October 1980

## ABSTRACT

The influence of surface waves on the Reynolds shear stress and the heat flux, measured in the atmospheric surface layer ~5 m above the ocean, is discussed using the method of Lu and Willmarth (1973). During the observational period, the phase velocity  $C$  associated with the dominant wave frequency is 33–80 times larger than the friction velocity  $u_*$ . When contributions to the momentum flux  $-uw$  are sorted out into the four quadrants of the  $(u, w)$  plane, the contribution from the interaction quadrants ( $u > 0, w > 0$ ;  $u < 0, w < 0$ ) increases as  $C/u_*$  increases. The contributions to the heat flux are not appreciably affected by  $C/u_*$ . While the probability that sweep and ejection quadrants associated with instantaneous shear-stress and heat-flux fluctuations occur at the same time is large and approximately independent of  $C/u_*$ , the probability of simultaneous occurrence of interaction events increases as  $C/u_*$  increases. The period between ejection events also increases with  $C/u_*$ .

## 1. Introduction

The mechanism of turbulent transfer of momentum and heat in the boundary layer adjacent to the ocean surface is somewhat different from that in the layer adjacent to the ground surface—a distinctive feature of the boundary layer over the water being the presence of moving waves. The influence of these waves on the turbulent surface layer must be assessed before making reliable estimates of the sea-surface stress, heat and humidity fluxes. Kitaigorodskii (1973) suggested that a relevant parameter that characterizes the dynamic interaction between sea and wind is the ratio  $C/u_*$ .  $C$  is the phase velocity corresponding to the dominant wave frequency  $n_0$  and  $u_*$  is the friction velocity  $-uw^{1/2}$ , where  $u$  and  $w$  are the longitudinal and vertical velocity fluctuations, respectively. Derivations of the normalized standard deviations  $\sigma_u/u_*$ ,  $\sigma_w/u_*$ ,  $\sigma_\theta/T_*$  ( $\theta$  is the temperature fluctuation and  $T_*$  the friction temperature  $w\theta/u_*$ ) from the behaviors suggested by Monin-Obukhov similarity have been considered by Volkov (1969) and others (e.g., Davidson, 1974). In particular, a significant increase in  $\sigma_u/u_*$  or  $\sigma_w/u_*$  was noted when  $C/u_*$  exceeded ~25.

Most of the observational evidence in the laboratory and atmosphere of the influence of water waves on the air flow above them has been in the form of spectra of velocity, pressure and, in a few cases, temperature and humidity fluctuations. Distinct

peaks in the power spectral densities of  $w$  and  $u$  have been observed (e.g., Benilov *et al.*, 1974) to occur at or near  $n_0$ , the frequency at which the spectral density of the surface-wave displacement is maximum. The data of Benilov *et al.* (1974) and Antonia and Chambers (1980) show that the  $uw$  cross spectrum indicates a relatively important transfer of momentum in the direction sea to air, at the wave frequency. Wave-induced contributions to  $-uw$  represented a reduction in  $-uw$  of ~25% when  $C/u_* \approx 80$ . Antonia and Chambers (1980) did not observe any appreciable change in the  $uw$  cospectrum when  $C/u_*$  was ~40. There is reasonable evidence, based mainly on observations in the laboratory, that wave-induced perturbations decay with height above the surface, with this decay rate depending on the relative magnitude of wind and wave speeds. While Elliott (1972) observed a noticeable peak in pressure spectra at  $n_0$ , there does not appear to be a detectable influence of waves on either temperature or humidity spectra. While Volkov (1969) noted that the generation of temperature (or humidity) fluctuations by the waves due to a fluctuating mean temperature (or humidity) gradient is unlikely to be important, the possible generation of temperature fluctuations from static pressure fluctuations was dismissed by Antonia and Chambers (1980).

Lu and Willmarth (1973) and Brodkey *et al.* (1974) examined the breakdown of the Reynolds stress according to the signs of the  $u$  and  $w$  signals obtained

in a turbulent boundary layer over a smooth wall. This technique was applied by Takeuchi *et al.* (1977) to  $u$  and  $w$  signals obtained in a boundary layer over mechanically generated water waves. Classification of events as ejections ( $u < 0, w > 0$ ), sweeps ( $u > 0, w < 0$ ), and wallward ( $u < 0, w < 0$ ) and outward ( $u > 0, w > 0$ ) interactions indicated that the events were more vigorous in the presence of relatively large-amplitude waves than over flatter surfaces. It should be noted that the interaction quadrants can be identified, in the case of a smooth surface, with the physical interactions, observed by Corino and Brodkey (1969), in which low-speed ejecting fluid is deflected back toward the wall while accelerated fluid is reflected away from the wall.

In this note, data examined by Antonia and Chambers (1980) using spectral techniques are re-examined using the technique developed by Lu and Willmarth, which is applied to the instantaneous products  $uw$  and  $\theta w$  measured at a nominal height of 5 m above the ocean surface from a stable platform in Bass Strait. The measurements were made for both relatively large ( $\sim 70$ – $80$ ) and small ( $\sim 40$ ) values of  $C/u_*$ , corresponding to conditions of appreciable and almost nonexistent influence of the waves on the  $uw$  cospectrum.

**2. Experimental details**

Measurements of  $u$ ,  $w$  and  $\theta$  were made from Kingfish B, the ESSO-BHP natural gas platform which stands in Bass Strait  $\sim 80$  km off the Gippsland coast of Victoria, Australia. The instruments for recording the above signals were mounted at a height  $z$  of  $\sim 5$  m above the mean water level (on a vertical pipe), supported at the end of a horizontal boom fastened to one of the western platform legs. A detailed description of the experimental arrangement, these instruments, their relative spatial location and the data handling techniques were given by Antonia *et al.* (1978) and Antonia and Chambers (1980). The horizontal velocity fluctuation  $u$  was obtained with a hot wire and the temperature fluctuation  $\theta$  was measured with a cold wire. The vertical velocity fluctuation  $w$  was obtained using a Gill propeller array, which also provided another measurement of  $u$ . The mean water level was continuously monitored with a resistance wave gage, which was suspended from the boom at a location 2 m downwind from the vertical mast to reduce the likelihood of wave-induced motion of the instrument mast.

Voltages proportional to  $u$ ,  $w$ ,  $\theta$  and humidity fluctuations ( $q$ ) were usually recorded on a four-channel Hewlett-Packard 3960 FM tape recorder. For a number of runs,  $\theta$  (or  $q$ ) was replaced by the surface displacement  $h$ . The humidity measurements are not discussed in this paper as during the early period of the experiment (when  $C/u_* \approx 80$ )

operational difficulties were encountered with the Lyman- $\alpha$  humidity meter and these were not overcome until later in the experimental period when  $C/u_* \approx 40$ . Moisture flux measurements have been discussed by Antonia and Chambers (1977), using the present technique, and by Antonia *et al.* (1978), and compared to momentum and heat fluxes. All runs discussed had a nominal 30 min duration except that for  $C/u_* = 38$  [run 3, Antonia and Chambers (1980), duration 58 min].

Spectra of the sea surface elevation (see Figs. 2 and 3 of Antonia and Chambers, 1980) were obtained at a number of different times throughout the observational period. The frequency of the main peak in the spectrum was found to be constant, equal to 0.13 Hz. Since the water depth at the platform is  $\sim 70$  m, the phase velocity  $C$  associated with the dominant wave was estimated using  $C = g/2\pi n$  (deep-water wave) and was equal to  $12 \text{ m s}^{-1}$ . The mean velocity at 5 m (see Fig. 1 of Antonia and Chambers, 1980), was always less than  $C$  for the entire experimental period, and for the major portion of the experiment the critical layer was close to or greater than 49 m [location of a propeller anemometer (Antonia *et al.*, 1978)]. The predominant waves were in the same direction as the wind.

The time constant of the  $w$  propeller is such that departure from the true and measured spectra of  $w$  occurs at  $k_{1z} \approx 2.5$  (Antonia *et al.*, 1978, Fig. 6). As the  $\overline{uw}$  and  $\overline{\theta w}$  values are expected to be underestimated by  $\sim 10\%$  only because of the  $w$  propeller response, a correction to account for the frequency response of the vertical Gill propeller was not attempted when considering the instantaneous products  $uw$  and  $w\theta$ .

**3. Results and discussion**

The laboratory technique of Lu and Willmarth (1973) has been applied to the atmospheric records of  $uw$  and  $w\theta$  for different values of  $C/u_*$ . Contributions to  $\overline{xw}$ , where  $x$  is  $u$  or  $-\theta$  from the four quadrants of the  $x, w$  plane, were computed as outlined by Lu and Willmarth (1973). The contribution to  $\overline{xw}$  from the region of the  $i$ th quadrant that lies outside the hole (hole size is set by the hyperbola  $|xw| = H\sigma_x\sigma_w$ ), is denoted by  $\overline{xw}_i(H)$ , such that

$$\frac{\overline{xw}_i(H)}{\overline{xw}} = \frac{1}{\overline{xw}} \lim_{T \rightarrow \infty} \frac{1}{T} \int_0^T xw(t) S_i(t, H) dt,$$

where  $i = 1$ ) outward interaction quadrant; 2) ejection quadrant; 3) wallward interaction quadrant; 4) sweep quadrant; and  $S_i(t, H)$  is an on-off function defined as

$$S_i(t, H) = \begin{cases} 1, & \text{when } |xw| > H\sigma_x\sigma_w \text{ and the} \\ & \text{point } (x, w) \text{ is in the } i\text{th quadrant} \\ 0, & \text{otherwise.} \end{cases}$$

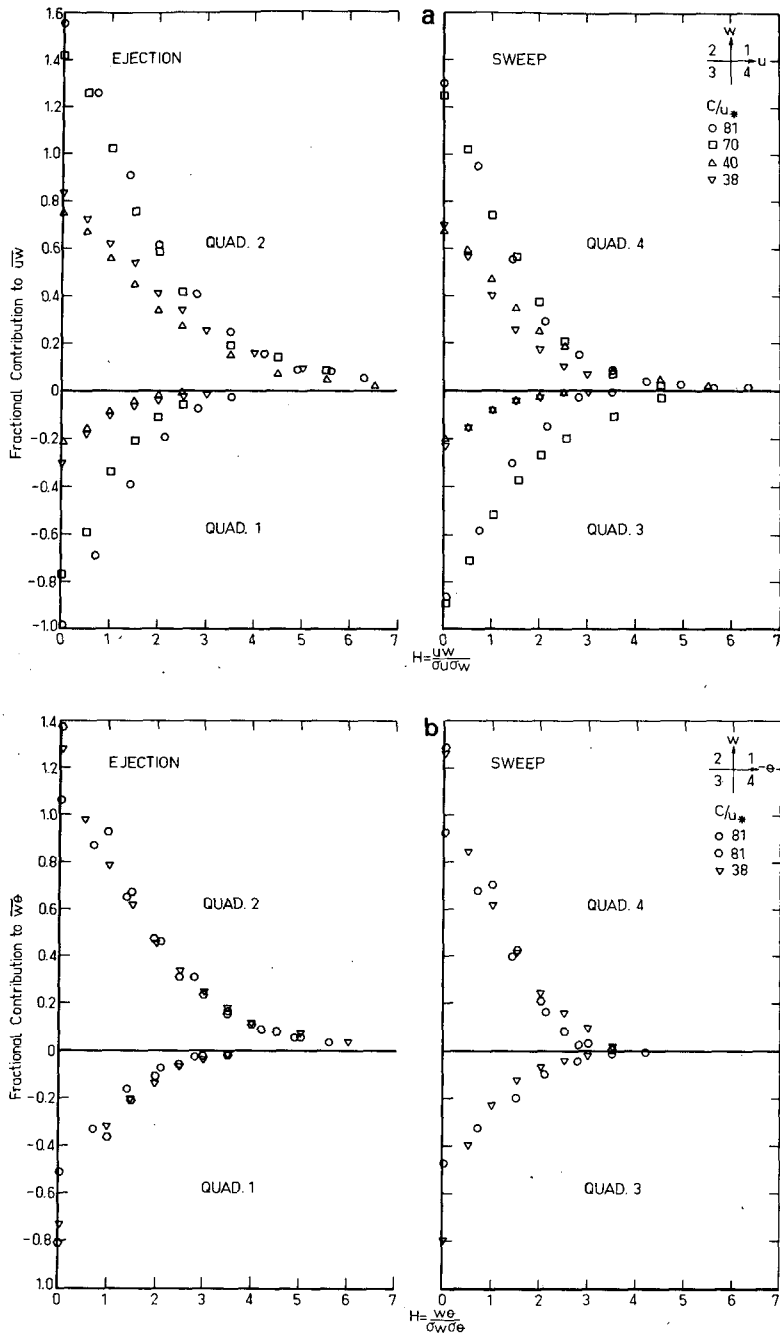


FIG. 1. Fractional contribution to  $\overline{xy}$  from the four quadrants in  $(x,y)$  plane. (a)  $x = u; y = w$ . (b)  $x = -\theta; y = w$ .

Values of  $\overline{xw}_i(H)/\overline{xw}$  for different values of  $H$  are shown for  $uw$  and  $w\theta$  in Figs. 1a and 1b. The values for  $C/u_* = 38$  are from Antonia and Chambers (1977). The behavior of the relative contributions from the different quadrants is qualitatively similar to that shown by Lu and Willmarth (1973). The contribution from the ejection quadrant remains larger than that from the sweep quadrant at all values of  $H$ ,

while contributions from the interaction quadrants are approximately equal. There is an apparent  $C/u_*$  dependence in the contributions from the different quadrants to  $-\overline{uw}$ , while the quadrant contributions to  $\overline{w\theta}$  appear essentially unaffected by the waves. The contributions  $\overline{uw}_i(H)/\overline{uw}$  appear more vigorous for all quadrants as  $C/u_*$  increases. The ratio of the contribution to  $-\overline{uw}(H = 0)$  at  $C/u_* \approx 80$  to that at

$C/u_* \approx 40$  is  $\sim 2$  for the sweep and ejection quadrants and 4 for the interaction quadrants.

Lu and Willmarth (1973) report that in the boundary layer over a smooth wall,  $\sim 80\%$  of the total Reynolds stress is due to ejections and  $60\%$  to sweeps, and each of the interaction quadrants contributes  $-20\%$ . This distribution is qualitatively similar to that in the  $uw$  results ( $H = 0$ ) with  $C/u_* \approx 40$ . The definition of ejection ( $H = 4.5$ ) and sweep events ( $H = 2.5$ ) used by Lu and Willmarth applies for  $uw$  when  $C/u_* \approx 40$ . At  $H = 2.5$ , the contribution to  $-uw$  from the interaction quadrants becomes negligible ( $<1\%$ ) while at  $H \approx 4.5$  the contribution from the sweep quadrant disappears. When  $C/u_* \approx 80$ ,  $H$  is nearly equal to 3.5 before the contribution to  $-uw$  from the interaction quadrants becomes small. The contributions to  $w\theta$  from interaction and sweep quadrants become small when  $H$  is equal to 3.0 and 4.0, respectively.

Takeuchi *et al.* (1977) found, from measurements in a wind-wave facility, that the introduction of a mechanically generated wave increases the fractional contribution to the measured  $-uw$  from each quadrant relative to values obtained only when wind waves are present.<sup>1</sup> The fractional increase is  $\sim 1.3$  for the sweep and ejection quadrants and 3 for the interaction quadrants, in agreement with the present results. Antonia and Chambers (1980, Fig. 2), found that a good inertial subrange could be identified in the  $u$  spectrum for  $C/u_* \approx 80$ , although a bump at the wave frequency did affect the start of the inertial subrange. They deduced that as the turbulence structure is not significantly influenced by the waves, the inertial dissipation technique should yield adequate estimates of the shear stress. The ratio of drag coefficients  $C_D$ , obtained by both direct and inertial dissipation<sup>2</sup> methods, was 0.5 and 1.0 for  $C/u_* \approx 80$  (one case) and 40 (three cases), respectively.

The reduction in the direct estimate of  $-uw$  may be partially attributed, in the time domain, to an increased activity in the interaction quadrants relative to the sweep and ejection quadrants, or, in the spectral domain, to the change in sign in  $Co_{uw}$  near the wave frequency. This change in sign was estimated by Antonia and Chambers (1980) to represent a reduction in  $-uw$  of  $25\%$  for  $C/u_* = 80$ .

It is possible to adjust  $-uw$  for  $C/u_* = 80$  to exclude the influence of the swell with the assumption that this influence is observed only in the interaction quadrants. It is clear from Fig. 1 that the increase

in activity, as  $C/u_*$  is increased from 40 to 80, is twice as large for the interaction as for the ejection and sweep quadrants. The reduction by 0.5 of the contribution from interaction quadrants to  $-uw$  (note that interaction quadrants make a negative contribution to  $-uw$ ) results in an apparent increase in  $-uw$  by a factor of 1.9. This value is consistent with the inertial dissipation estimate of the shear stress by Antonia and Chambers (1980). On the basis of the above assumption, renormalized contributions to  $-uw$  (for  $H = 0$ ) from the various quadrants by the Reynolds shear stress are equal to 0.8, 0.68 and  $-0.48$ , respectively, for the ejection, sweep and interaction quadrants. These contributions are in reasonable agreement with those obtained when  $C/u_* \approx 40$ . It is possible that the shear stress estimates using the direct  $-uw$  measurement and the inertial dissipation measurement are perhaps both "correct." A discussion on the relative merits of the cross-correlation and dissipation methods of evaluating the surface fluxes is given by Antonia *et al.* (1978). The inertial dissipation estimate yields a shear-stress value that would apply in the absence of swell, as it is obtained from the  $u$  spectrum at frequencies greater than that of the predominant wave, where the turbulent structure should not be significantly influenced by the wave. The direct  $-uw$  estimate is a measure of the total stress at the surface, which will include the influence of the predominant wave. For  $C/u_* \approx 80$ , a transfer of momentum in the direction water to air is suggested (Antonia and Chambers, 1980, Figs. 4a and 5a).

It is useful to compare the joint probability of occurrence of signals such as  $uw$  and  $w\theta$  in the various quadrants of the  $xw$  plane ( $H = 0$ ), as this information will provide information on the similarity between fluctuations  $uw$  and  $w\theta$ . The conditional probability  $P(\alpha_i/\beta_j)$  is used here to denote the probability that the event  $\alpha$  in the  $i$ th quadrant occurs whenever event  $\beta$  in the  $j$ th quadrant has already occurred ( $i, j = 1, 2, 3, 4$ ). The conditional probability  $P[(uw)_i/(w\theta)_j]$  is equal to

$$\begin{pmatrix} 0.68 & 0.28 & 0 & 0 \\ 0.32 & 0.72 & 0 & 0 \\ 0 & 0 & 0.68 & 0.32 \\ 0 & 0 & 0.32 & 0.68 \end{pmatrix}$$

and

$$\begin{pmatrix} 0.55 & 0.28 & 0 & 0 \\ 0.45 & 0.72 & 0 & 0 \\ 0 & 0 & 0.47 & 0.27 \\ 0 & 0 & 0.53 & 0.73 \end{pmatrix}$$

for  $C/u_*$  equal to 81 and 38, respectively. The con-

<sup>1</sup> For the mechanically generated wave  $U/C > 1$ , the wave-induced perturbations are removed, and the ratio of the wave perturbation to  $-uw$  is  $\sim 0.5$  and represented a transfer of momentum in the direction of water to air.

<sup>2</sup> A Kolmogorov constant of 0.5 was assumed (Antonia *et al.*, 1978).

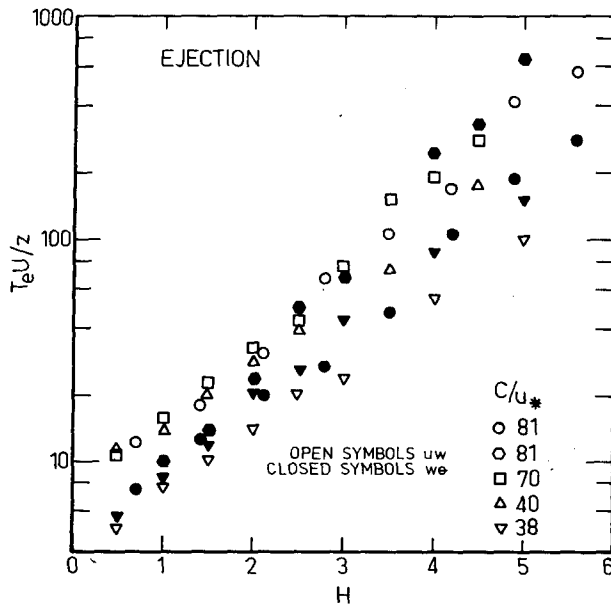


FIG. 2. Mean period between ejections as a fraction of hole size.

vention here is that subscripts  $i$  and  $j$  denote the positions of the rows and columns, respectively. It is clear from these probability arrays that for  $C/u_* = 38$ , the dominant elements are  $P(\alpha_2/\beta_2)$  and  $P(\alpha_4/\beta_4)$ , whereas for  $C/u_* = 81$ , all diagonal elements dominant.

The mean values of the time between ejection  $T_e$  and sweep  $T_s$  events are shown as a function of  $H$  in Figs. 2 and 3. There does appear to be a difference in distributions of  $T_e$  and  $T_s$ , associated with  $uw$ , for different  $C/u_*$ . Fewer events appear to occur when  $C/u_* \approx 80$  than when  $C/u_* \approx 40$ . With  $H \approx 4.5$ , an average value of  $T_e U/z$  is 120 ( $C/u_* = 40$ ) and 230 ( $C/u_* = 80$ ) while for  $H = 2.5$ ,  $T_s U/z \approx 40$  ( $C/u_* = 40$ ) and 80 ( $C/u_* = 80$ ). These differences are at variance with the observation by Lu and Willmarth (1973) that  $T_s = T_e$ . If, for  $C/u_* = 80$ , the sweep event were defined by  $H = 3.5$ , then  $T_s U/z \approx 280$ , which would be in reasonable agreement with the mean time between ejections.

The  $T_e$  and  $T_s$  distributions, associated with  $w\theta$ , are not so convincing as those for  $uw$  on account of the large difference between the two  $T_e$  distributions when  $C/u_* \approx 80$ . The effect of  $C/u_*$  on these distributions, however, is qualitatively similar to that observed in the case of  $uw$ . With the Lu-Willmarth criteria used to define sweep and ejection events, values of  $T_s U/z$  and  $T_e U/z$  for  $w\theta$  are similar to those obtained for  $uw$ . A minor modification of the definitions for the sweep ( $H = 3.0$  instead of 2.5) and ejection ( $H = 4.0$  instead of 4.5) events would cause  $T_s$  and  $T_e$  to be approximately equal.

The frequency of ejection events is  $\sim 1 \text{ min}^{-1}$  ( $T_e U/z = 120$ ) for  $C/u_* \approx 40$  and  $0.25 \text{ min}^{-1}$  ( $T_e U/z = 230$ ) for  $C/u_* \approx 80$ . When examining features of

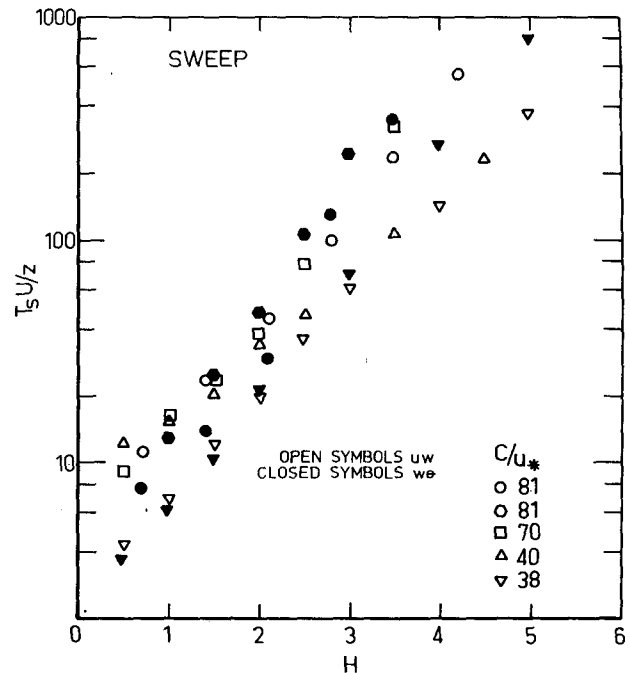


FIG. 3. Mean period between sweeps as a fraction of hole size.

the organized motion in the atmospheric surface layer, Phong-anant *et al.* (1980) found that contributions of the ramp events to  $w\theta$  and  $-uw$  were 3 and 8%, respectively, in the range  $-0.03 \leq z/l \leq -0.001$ . Thus any mechanism which tends to break up the organized turbulent motion when  $z/L$  is small would have a detectable effect on the Reynolds stress but only a slight effect on heat flux.

**Acknowledgments.** We acknowledge the generous cooperation of Dr. I. S. F. Jones, Royal Australian Navy Research Laboratory, and ESSO/BHP. We are also indebted to Drs. D. Britz, C. A. Friehe, S. Rajagopalan and K. R. Sreenivasan for their assistance with the experiment and data reduction.

The research was supported by the Australian Research Grants Committee.

#### REFERENCES

- Antonia, R. A., and A. J. Chambers, 1977: Similarity of Reynolds stress, heat and moisture fluxes in marine boundary layer. *Proc. 6th Australasian Hydraulics & Fluid Mechanics Conf.*, Adelaide, Part I, 41-44.
- , and —, 1980: Wind-wave induced disturbances in the marine surface layer. *J. Phys. Oceanogr.*, **10**, 611-622.
- , —, S. Rajagopalan, K. R. Sreenivasan and C. A. Friehe, 1978: Measurements of turbulent fluxes in Bass Strait. *J. Phys. Oceanogr.*, **8**, 28-37.
- Benilov, A. Y., O. A. Kuznetsov, and G. N. Panin, 1974: On the analysis of wind wave-induced disturbances in the atmospheric turbulent surface layer. *Bound.-Layer Meteor.*, **6**, 269-285.
- Brodkey, R. S., J. M. Wallace and H. Eckelmann, 1974: Some properties of truncated turbulence signals in bounded shear flows. *J. Fluid Mech.*, **63**, 209-224.

- Corino, E. R., and R. S. Brodkey, 1969: A visual investigation of the wall region in turbulent flow. *J. Fluid Mech.*, **37**, 1–30.
- Davidson, K. L., 1974: Observational results on the influence of stability and wind-wave coupling on momentum transfer and turbulent fluctuations over ocean waves. *Bound.-Layer Meteor.*, **6**, 305–331.
- Elliott, J. A., 1972: Microscale pressure near waves being generated by the wind. *J. Fluid Mech.*, **54**, 427–448.
- Kitaigorodskii, S. A., 1973: *The Physics of Air-Sea Interaction*, A. Baruch, transl., P. Greenberg, Ed. Israel Program for Scientific Translation, Jerusalem, 237 pp.
- Lu, S. S., and W. W. Willmarth, 1973: Measurements of the structure of the Reynolds stress in a turbulent boundary layer. *J. Fluid Mech.*, **60**, 481–511.
- Phong-anant, D., R. A. Antonia, A. J. Chambers and S. Rajagopalan, 1980: Features of the large-scale motion in the atmospheric surface layer. *J. Geophys. Res.*, **85**, 424–432.
- Takeuchi, K., E. Leavitt, and S. P. Chao, 1977: Effects of water waves on the structure of turbulent shear flow. *J. Fluid Mech.*, **80**, 535–559.
- Volkov, Y. A., 1969: The spectra of velocity and temperature fluctuations in airflow above the agitated sea surface. *Izv. Atmos. Ocean. Phys.*, **5**, 1251–1265.

## Sea-Air Heat and Freshwater Fluxes in the Drake Passage and Western Scotia Sea<sup>1</sup>

ALBERTO R. PIOLA<sup>2</sup>

*Servicio de Hidrografía Naval, Buenos Aires, Argentina*

DANIEL T. GEORGI

*Woods Hole Oceanographic Institution, Woods Hole, MA 02543*

10 July 1980 and 29 September 1980

### ABSTRACT

Hydrographic data from the vicinity of the Antarctic Polar Front in the Drake Passage and the western Scotia Sea are used to estimate the heat content and salinity differences for the upper ocean between summer and winter. Assuming that these differences are caused primarily by the exchange of heat and freshwater at the sea surface during the 6-month period from February to July, an integrated heat flux of  $11.3 \pm 5.2 \times 10^8 \text{ J m}^{-2}$  ( $2.69 \pm 1.24 \times 10^4 \text{ cal cm}^{-2}$ ) and an excess of precipitation of  $276 \pm 190 \text{ mm}$  are required. These fluxes agree well with estimates derived from historical meteorological observations.

### 1. Introduction

It is important to investigate the seasonal variation of upper-water-column properties to evaluate the possible role of ocean-atmosphere interactions in various water-mass formation mechanisms (McCartney, 1977; Georgi, 1979). Hydrographic data from the Drake Passage and western Scotia Sea are used to estimate the variation of temperature and salinity in the upper ocean between summer and winter. These values are then used to compute heat and fresh-water fluxes, which are compared to estimates derived from meteorological observations. Because selected summer-winter station pairs are presumed to fall along streamlines of the Antarctic Circumpolar Current, changes in heat content and salinity due to horizontal advection are eliminated.

Based on water-mass properties and the vertical structure of temperature and salinity, the upper waters of the Drake Passage and western Scotia Sea

can be subdivided into four distinct zones: the Subantarctic Zone, the Polar Front Zone, the Antarctic Zone, and the waters within and south of the Weddell-Scotia Confluence (Gordon *et al.*, 1977; Whitworth, 1980). With current-meter and hydrographic data, Nowlin *et al.* (1977) have shown that the transition regions between these zones are associated with relatively high velocity cores of the Antarctic Circumpolar Current. In the upper waters, these cores are associated with water-mass fronts characterized by relatively large horizontal, primarily meridional, property gradients and multiple temperature and salinity inversions (Gordon *et al.*, 1977; Georgi, 1978; Joyce *et al.*, 1978). The geographic location of the fronts is not fixed. Large shifts occur when rings are formed (Joyce and Patterson, 1977) and when wavelike disturbances pass through the region (Legeckis, 1977). Sievers and Emery (1978) documented a meridional shift of 150 km in three weeks with expendable bathythermograph data. Due to the time variability of the Antarctic Circumpolar Current, two stations in the same geographic position will not have the same oceanographic characteristics. Thus, comparison of stations in the same geographic location could confuse heat and salt content

<sup>1</sup> Woods Hole Oceanographic Institution Contribution No. 4681.

<sup>2</sup> Present affiliation: Woods Hole Oceanographic Institution, Woods Hole, MA 02543.